Toward Computing with Spider Webs: Computational Setup Realization

S.M.Hadi Sadati and William Thomas

University of Bristol, Department of Engineering Mathematics,
Bristol BS8 1TH, U.K.
s.m.hadi.sadati@bristol.ac.uk, wt13103@my.bristol.ac.uk

Abstract. Spiders are able to extract crucial information, such as the location prey, predators, mates, and even broken threads from propagating web vibrations. The complex structure of the web suggests that the morphology itself might provide computational support in form of a mechanical signal processing system - often referred to as morphological computation. We present preliminary results on identifying these computational aspects in naturally spun webs. A recently presented definition for physical computational systems, consisting of three main elements: (i) a mathematical part, (ii) a computational setup with a theoretical and real part, and (iii) an interpretation, is employed for the first time, to characterize these morphological computation properties. Signal transmission properties of a real spider orb web, as the real part of a morphological computation setup, is investigated in response to step transverse inputs. The parameters of a lumped system model, as the theoretical part of a morphological computation setup, are identified empirically and with the help of an earlier FEM model for the same web. As the possible elements of a computational framework, the web transverse signal filtering, attenuation, delay, memory effect, and deformation modes are briefly discussed based on experimental data and numerical simulations.

Keywords: Morphological Computation, Spider Web, Vibration, Lumped System Model, Signal Processing.

1 Introduction

The spider's web is a complex structure created by a dedicated and interactive behavior pattern optimized through evolution over many million years to serve the ultimate purpose of catching prey [1, 2]. The efficacy of the web as a trap depends heavily on the correct and robust categorization and localization of various events, including trapped prey, potential mates, broken threads, wind, and others. Somehow spiders are capable of categorizing and locating events robustly based on a very small amount of information that is only locally available. This suggests that the web might not be only a passive catching device, but rather contributes to the pattern recognition task. In this research, we propose a theoretical framework toward understanding how spiders may use their web as a computational device for the aforementioned purposes.

The typical spider's orb web consists of a capture spiral which radiates from the center, held by several radial threads (Fig. 2.left) [1]. The radial threads are built using dragline silk, an exceptionally tough material with high tensional strength, which provides the framework of the web [3]. The role of the spiral is to capture prey, benefiting from its sticky thread and large strain elasticity that creates a strong and effective snare, capable of capturing large prey relative to the web [4]. Typically, orb-weaving spiders have poor eyesight and in consequence are heavily dependent on (i) web vibrations, to provide information on current surroundings [4], and (ii) highly sensitive mechanoreceptors on all eight legs [5,6], which together enable the animal to interpret propagating web vibrations [7, 8]. The structural [9, 10] and vibration properties [5, 11, 12] of the spider web has been studied extensively . Mortimer et al. have recently studied and summarized the relevant research on the relationship between material properties of the web and its ability to transmit vibrations in experiments and finite element modeling, [7,8]. The following elements are proposed as control mechanisms that the spider employs in order to influence the structure sonic properties such as speed and amplitude [7, 8]: super-contraction, web tensioning, and altering longitudinal (along with the threads), lateral (perpendicular to threads in web plan) and transverse (perpendicular to threads and web plan) vibrations. However, modal behavior of a spider orb-web-like, but not quite similar, structure is studied recently for designing an acoustic metamaterial [13].

Taking all this into account the spider web can be perceived as a highly dynamic, morphological computation device. Moreover, an externalized computational resource that the spider is able to build on demand. The concept of outsourcing computation to a physical body (e.g., from the brain to another part of the body) is usually referred to as morphological computation [14–18] and can be observed in biological systems at different scales [19]. Examples of benefiting from structural natural behavior by design for simplifying or improving a task [20], replacing computation units in a traditional computation framework with morphological counterparts [18, 21], and emerging adaptive behavior from simple morphological rules [22] are mentioned as candidates for morphological computation. Hauser et al. presented two theoretical frameworks for the concept [17, 18], realized in robotic research [15, 16, 22], where the highly non-linear reservoir in a reservoir computing paradigm is substituted with a complaint body, reducing a complex problem of dynamic filter design or system limit-cycle control to dynamic learning of a set of linear weights. Ghazi-Zahedi et al. have investigated quantitative measures for morphological computation in continuous and discrete systems [23,24]. A summary of the most current state of the art, definitions, and examples of morphological computation is presented by Füchslin et al. [25]. However, a fundamental approach for designing by definition and even identifying instances of morphological computation is not yet presented or agreed upon. However, a good starting point might be employing the methods discussed in the theoretical physics and computer science research on the definition and modeling of a computing physical phenomenon [26, 27], despite their differences [25]. For the first time in this study, we try to extend a recently

proposed definition for physical computational systems by Giunti [27], (i) to define morphological computational systems, and (ii) to realize the computational capability of a natural structure, i.e. spider webs.

This paper is structured as follows. Materials and methods are presented in Section 2. There, the adopted definition for a morphological computation setup is discussed. The experimental procedure used by Mortimer et al. [7,8] is explained. A mathematical lumped mass-spring-damper system model, similar to [9] by using the parameters in [7,8,11], is derived, as the theoretical part for a morphological computation setup. Empirical and numerical results are compared and discussed in Section 3. The experimental data set is used to investigate signal processing features such as arrival times (delay), attenuation, frequency filtering, memory effect, and assessing their variation with input location, to realize the web structure behavior, as the real part of a morphological computation setup. A conclusion is presented in Section 4.

2 Materials and Methods

2.1 Morphological Computation System Realization

Giunti [27] has proposed a precise analysis for physical realization of a computational system, by looking at the modeling relation between a dynamic system and phenomena, as a complex object. A computational system contains three parts (Fig 1.a); 1) a mathematical part in the form of a discrete n-component dynamic system ($DS = (M, (g^t)_{t \in T})$) with a state space ($M$), a transition function (g^t) and a time set (T); 2) a computational setup ($H = (F, B_F)$) with a theoretical part (F) and a real (physically feasible) part (B_F); and 3) an interpretation ($I_{DS,H}$) linking the aforementioned parts. Despite the similarity to empirically correct dynamical models for physical phenomena, e.g. modeling a spider orb-web dynamics in this research, a computational system is proved different by characterizing a form of purely theoretical (a-priori) interpretation of the mathematical part on the setup part. This interpretation can be only established empirically (a-posteriori) for models derived to understand phenomena in empirical science. Fig. 1.b presents an example of a computational task, consisting of an operation and a memory, calculated with a physical computational setup. The mathematical dynamic system part has two discrete components, a memory, and an operation, interpreted to the theoretical part of the physical computational setup which is an ideal representation of the setup real part. The calculated result by the setup real part is matched with a state of the theoretical physical model, which is then interpreted back to a state in the task mathematical part. We dismiss the exact characteristics and relations of different parts of this definition at the moment to focus on our extension to a morphological computation system.

In a morphological computation system, the setup part (H) has a theoretical model for the physical setup (F), e.g. the lumped system dynamic model for the web, and the real behavior of the web (B_F), which are the physically feasible realizations of the theory. Distinct behaviors observe in the setup empirically, e.g.

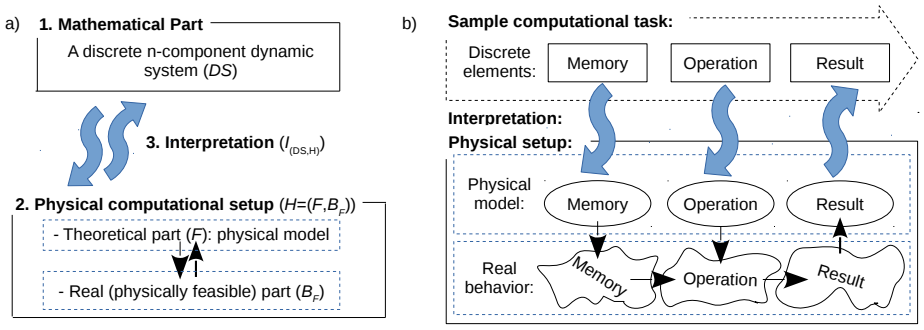

Fig. 1. (a) Three elements of a physical computational setup, (b) implementation of a sample computational task, consisting of an operation and a memory element, on a physical computational system.

signal filtering, delay, memory effect, deformation modes, etc., are an F-realizer if a close enough theoretical model can be presented for it in F. These distinct behaviors indicate that the setup posses discrete behavior, to switch between, as means of discrete programming to be interpreted by a proper dynamic system DS. As an example, a signal processing task can be programmed as a discrete sequence of filtering, deformation modes and memory of a few previous time steps, subject to availability and realization of a proper dynamic system DS and an interpretation I. Despite a man-made computational device with pre-known systems, computational capabilities of a natural morphological computation setups need to be identified, either in real experiments or based on verifiable predictions from numerical simulations. As a result, not only I and DS, but identification and proper formulation of the H is a challenge too.

To realize the spider web as a physical computational setup, we assert that (i) the web structure serves as the real part of a computational setup (B_F), and (ii) the theoretical part of the setup (F) is a mathematical model for the structure dynamics, e.g. the lumped system model presented here. In this study, we try to realize the properties of the web with possible computational capability in experiments and numerical simulations. The possible dynamic system (DS) and interpretation (I) parts are going to be investigated in a future study.

2.2 Experiments on Spider Orb-web

Experimental data were recorded from an orb-web of a Garden Cross Spider Araneus diadematus, which typically positions itself at the hub (Fig. 2.left) [7]. Four points along seven radii of the web were excited, five times each, with a 3 ms duration and 170 μm amplitude square wave input, using a solenoid positioned perpendicular to the structure (transverse direction). Two Laser Doppler vibrometers were used to record both the input signal delivered to the web at four positions along seven radii (Polytec PDV-100) and a unique output response near the hub (Polytec PSV-400), see [7].

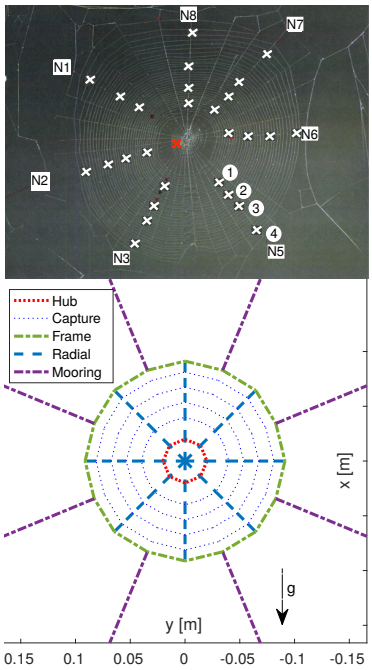


```
for i_c = 1 : 6  { iterate over circular webs
  for i_ϕ = 1 : 16 { iterate over radii and middle spiral masses
    i_b = (i_c-1)*16 + i_ϕ + 1 ; body counter
    i_k = i_k + 1 spring numerator,
    body(i_b).type = 'rigid' ; body type
    body(i_b).m = nC_n ρ a l ; body mass
    body(i_b).I_com = [ 0, 0, 0 ] ; body COM position in local frame
    joint(i_k).first = 0 ; DOF Joint 1st body
    joint(i_k).second = i_b ; DOF joint 2nd body
    joint(i_k).tr(1).trans = [ inf, inf, inf ] ; 3D translational DOFs only
    joint(i_k).dof(1).init = x_(i_ϕ,i_c) ; 1st DOF initial position
    joint(i_k).dof(1).damp.visc = ν_m ; 1st DOF viscous damping
    ... similar for 2nd and 3rd DOF
    i_k = i_k + 1,  i_p = ... previous mass number
    joint(i_k).first = i_p; spring 1st body (previous body)
    joint(i_k).second = i_b ; spring 2nd body (current body)
    joint(i_k).tr.trans = [ 0, 0, 0 ] ;
    joint(i_k).tr.rot = [ 0, 0 ] ; location & orientation in 1st body
    joint(i_k).tr2nd.trans = [ 0, 0, 0 ] ;
    joint(i_k).tr2nd.rot = [ 0, 0 ] ;  location & orientation in 2nd body
    joint(i_k).spring.coeff = nC_n Ea/(C_c l); spring coefficient
    joint(i_k).spring.init = C_c l; spring initial length
    joint(i_k).damp.visc = nC_n ν_l/(C_c l) ;
    if mod( i_ϕ , 2 ) == 1 { no radial spring for middle spiral thread masses
      joint(i_k).spring.coeff = 0 ; joint(i_k).damp.visc = 0 ; }
    i_k = i_k + 1,  r = [x, y, z]_(i_ϕ+1,i_c) − [x, y, z]_(i_ϕ,i_c); spiral spring vector
    l_s = sqrt( r.r^T ) ; spiral spring length
    ... same as above for spiral springs } }
```

Fig. 2. (left) Labeled experimental spider orb-web and top view of 3D Lumped system model. The nodes represent lumped masses and different lines represent the model springs/dampers (right) Sample Matlab code inputs for AutoTMTDyn package as in [28]. The model source code is available from [29].

2.3 Lumped System Model:

The web is modeled as a mass-spring-damper network [9] with 8 radii and 6 circular webs to capture all the experimental points (Fig. 2.left). Point masses are assumed at the nodes and middle of the circular webs, to capture the thread second deformation modes and simulate the secondary outer frame as in [10], with Cartesian motion of the masses as generalized coordinates (q). AutoTMTDyn Matlab package [28] is used to derive the system constrained Lagrange dynamics in a vector formalism in the form

$$M\ddot{q} + N_{\mathrm{m}}\dot{q} + L_{,q}^{\mathrm{T}}(N_{\mathrm{l}}L_{,q}\dot{q} + K\Delta L) + Mg = \lambda,\ q_{\mathrm{in}} = u, \tag{1}$$

where M is the mass matrix, N_{m} is the lateral damping matrix, N_{l} is the longitudinal damping matrix, L is the springs' vector, $\Delta L = L_{,q}q - C_{\mathrm{c}}l_0\hat{L}$ is their deformation vector, K is the stiffness coefficient matrix, g =9.81 m/s^2 is the gravity, u is the input signal, λ is a Lagrange multiplier resulting from the input constraint, q_{in} is the generalized coordinate on which the input signal is exerted, $\dot{x} = \partial x/\partial t$ for the time derivatives, and $y_{,x} = \partial y/\partial x$ for the spatial derivatives. λ, i.e. a constrained dynamic system, is used to match the experiments excitation in numerical simulations since it is hard to measure input force on the web

and only the displacement imposed at the excitation location can be observed accurately. Modeling parameters are extracted from the experimental measurements and [7,11]. Threads diameter (r- 1.2 μm), number of strands (n- radial: 3, mooring, hub, outer frame: 4, capture 2), elasticity modulus (E- capture: 0.06, others: 4 [GPa]), density (ρ- 1300 Kg/m^3, and web dimensions (l_0- hub, free zone: 20, capture zone segments: 11.2, outer frame: 10, mooring 90 mm). The masses ($m = \rho a l,\ a = n\pi r^2$) are calculated based on the adjutant segments initial length ($l = C_c l_0$). The threads elastic coefficient is found from Hook's linear stress-strain relation for axial elongation ($k = Ea/l$ N/m) and the thread average initial stresses (radial: 458, capture: 2.25 μN) reported by Masters [12] are used to calculate supercontraction ratios ($C_{\rm c}$- radial: 99.7%, capture: 99%) and unloaded thread lengths. The thread lateral damping ($\nu_{\rm m}$, exerting on masses) is a summation of Stokes' air drag ($\nu_{\rm d} = 6\pi\nu_{\rm air},\ \nu_{\rm air}$ =1.81e-5 Kg/(ms)), valid for very low Reynolds numbers (here $Re \approx$4e-3$\ll$1), and thread deflection damping ($\nu_{\rm thread}$ =1.8e-5 Kg/(m.s)) [11], all per unit length. The radial thread longitudinal damping ($\nu_{\rm l_r}$- exerting on connecting springs.), is the only free parameter which is identified to be 8e-8/l N/m (proportional to thread elastic coefficient with dimension N/m), for the best agreement between the maximum transverse deflection in numerical simulation and experiments. The linear part of the system in Eq. 1 (for $l_0 = 0$) is a proportionally damped system if $\nu_{\rm l_c}$ for capture thread is proportional with E as $\nu_{\rm l_c} = \nu_{\rm l_r} E_{\rm c}/E_{\rm r}$. Two corrections coefficients are considered to be multiplied by n; $C_{\rm n}$ which is the ratio of the number of threads in the experiments to that in the model (hub: 7, radial: 4.625, mooring 1.875, capture; 7.75), and $C_\phi = 0.216$, which is due to the reduced angle between the capture and radial threads in the model. Parts of the code used to model the web in AutoTMTDyn package is presented in Fig. 2.right. The discussed parameters in this section are used in the input code too. The model source code is available from [29]

3 Results and Discussion

The time series and Fast Fourier Transfer (FFT) of the average of all input signals, plotted in Fig. 3.a, are used in this study. Experimental and simulation time series for N2 (same thread as output, compare Fig. 4.c) and N6 (opposite side of the net) are compared in Fig. 3.b,c. The simulation results for the input response has less accuracy on the opposite side of the web (Fig. 4.c), based on the simulation and experimental signal maximum values. Overall damping is stronger in the simulations where sharper peaks are observed. Smaller variation in maximum signal amplitude of different experiments shows less lateral damping along radial threads. A large hysteresis is observed in some experimental results where the output signal settles with an offset from the initial equilibrium point. The web nonlinear damping and structural hysteresis need further investigation in a future study. The experimental signal Bode diagram for input-output gain (Fig. 3.b,c) shows large damping values for low-frequency (1-500 Hz) responses, perhaps to cancel wind and rain disturbances. A smooth response for

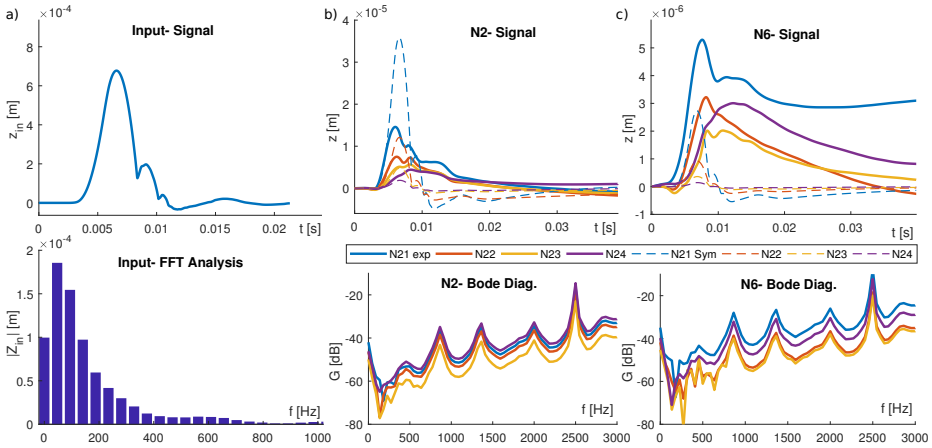

Fig. 3. Experimental results: (a) Input signal time series and FFT diagram, experimental and simulation time series and Bode gain diagram results for inputs on (b) N2 and (c) N6. The model thread longitudinal damping (ν_{l_r}) is identified to minimize the max error between the simulation (dash lines) and experimental (solid lines) result time series (b,c- top).

frequencies more than ≈1000 Hz, perhaps to match the natural frequency of the spider's prey wingbeats [11], is observed that may suggest reduced noise to signal ratio for high-frequency signals. High gain for the bias value (0 Hz) in Bode diagrams shows some overdamped vibration modes (mostly with low frequency), suggesting some memory effect in the continuous signal, meaning that the effect of a low-frequency excitation remains in the structure for some time, while some modes are not filtered out completely, perhaps enabling the spider to exploit useful information from the resultant vibrations. However, the lack of positive correlation between the maximum normalized displacement of different experiment trials at each location shows the elastic behavior of the structure with no memory effect (plastic deformation) in maximum absolute deformation values, neglecting the signal bias, between the trials (Fig. 4.b). Fig. 4.b shows antiphase response for excitation on the same side of the net (N11 and N21) but in phase response for the opposite side, that suggests the shape of the web dominant deformation mode for, probably, frequencies of 500-1000 Hz. Signal propagation delay in Fig. 4.c is defined as the time that takes the output signal to reach its maximum, measured from the start of the input signal. Fig. 4.c shows high tension pathways along N2, 3, 7 and 8, probably due to the web weight in vertical orientation, have higher wave speed, similar to the observations in [11].

Longitudinal waves (Fig. 5.a,b) rather than lateral waves (Fig. 5.c) are arguably the potential key for spider signal processing due to (i) higher signal to noise ratio and (ii) lesser sensitivity to environmental disturbance [7,8]. The longitudinal waves should be measured along the threads (local frame) (Fig. 5.a) rather than along the threads projection on the initial web plan (i.e. w.r.t. an

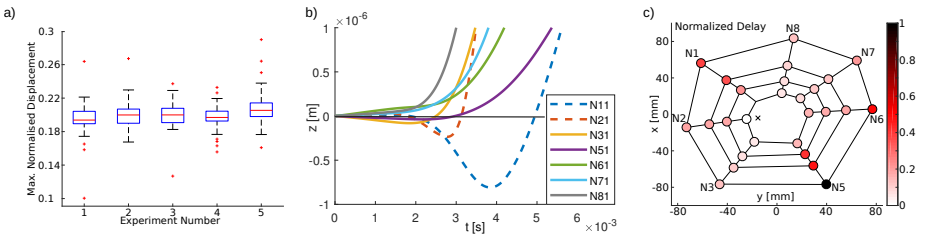

Fig. 4. Experimental results: (a) Maximum normalized deformation for different locations along the web in different experimental trials, showing no memory effect between different experiment trials. (b) Arrival output signals from spiral 1, showing antiphase deformation of the hub on the excitation side of the web and in phase deformation on the opposite side of of the web. (c) Normalized signal delay to reach maximum value for different input locations, showing the signal propagation pattern.

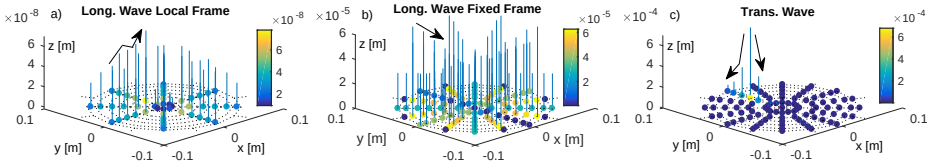

Fig. 5. Simulation results for input at N22: Longitudinal wave maximum value (a) amplifies along the threads toward the web hub but (b) looks decaying if measured w.r.t. an external fixed frame. (c) Transverse wave maximum value at the excitation point. Arrows show the values' change trend along a radial thread, bars height and their root point color indicate the deformation values.

externally fixed reference frame) (Fig. 5.b). This makes their experimental investigation challenging since it is easier to measure the later one with a fixed laser vibrometer, while onboard sensors, i.e. a spider itself, on the structure are needed to measure the former one. Simulations show longitudinal signal amplification toward the free zone (Fig. 5.a), the gap between the hub and the capture zone with no spiral threads, despite lateral waves that are largely damped toward the hub (Fig. 5.c) and prone to noises [7, 11].

The discussed model is better in capturing signal maximum amplitudes compared to the FEM model results in [7]; however, the frequency domain responses still presents significant differences compared to the experimental results. We aim to improve our model to capture the actual web spectral behavior and to investigate the Bode diagram differences between the simulation and experimental data (Fig. 6.a), which can be used to investigate the web hysteresis and damping behavior. This helps with more accurate predictions for the spectral behavior of the longitudinal waves that seem to poses stronger signal filtering capability based on our preliminary results (Fig. 6.b). Besides, our simulations show antiphase deformation mode (Fig. 6.c), similar to the experiments (Fig. 6.a), but for unrealistic high frequencies ($\approx$ 130 KHz) that needs further investigation.

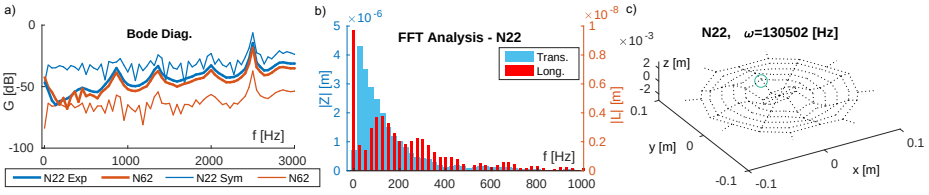

Fig. 6. Simulation results for input at N22: (a) Bode gain diagram from simulations and experiments for N22 and N62, showing smoother frequency response with less damping for low frequency domains and along the radial thread in the experiments compared to the simulations. (b) Comparison of FFT analysis results for transverse and longitudinal waves based on simulation results, that shows a highly damped lateral vibration with less contribution of the high frequency modes for the lateral wave, but a distinguishable transfer function with a modal damping pattern for the longitudinal wave frequency response. (c) A mode shape with antiphase deformation of the hub w.r.t. the excitation signal.

While we try to preserve the theoretical simplicity and clarity of the model, to remain useful as the theoretical part in a computational setup definition, we plan to investigate high fidelity methods such as cyclic symmetric, membrane, and finite element models in the future. An artificial web will be fabricated to further investigate our hypothesis and predictions, and to be used as a morphological computational setup for signal processing with application in designing new vibration and flow sensors.

Our experimental and modeling effort show the possibility of identifying and theoretically realizing the computational properties of the spider web as a morphological computational setup. Preliminary results suggest that we should exploit properties like memory, signal filtering, delay, amplification, and attenuation as computational elements and interpret them (I) as meaningful elements of a computational paradigm (DS). As a candidate for such computational paradigm (DS) and interpretation (I), we plan to follow the theoretical foundation for morphological computation presented by Hauser et al. [18]. Their proposed theories established that the nonlinearity and memory effect in a high dimensional (sufficiently rich) dynamic system (H- the computational setup), e.g. compliant body robots, can partly characterize a nonlinear, time-invariant filter with fading memory in the form of a Volterra series (DS- Dynamic System). The interpretation (I) is established since a Volterra series can characterize (i) a nonlinear time-invariant filter with fading memory (DS), as well as (ii) any continuous nonlinear dynamic system (H). Such morphological filter is able to emulate arbitrary input-output mappings in continuous time by adopting a simple linear readout. In this sense, the spider web may serve as a morphological computational device to generate fading memory response to external signals. Alternatively, Hauser et al. [17] have extended this theory to autonomous generation of a large diversity of periodic movements by providing feedback into the morphological computing system, which is verified in soft robotic studies [16,22].

As a candidate, a generic nonlinear stable limit cycles equation is chosen in [17] as the system target (DS) describing a stable nonlinear limit cycle. The interpretation (I) is established by (i) showing that the computational setup theoretical part (BF) is feedback linearisable (has a feedback equivalent linear system), and (ii) employing a transfer function and a specific feedback to map this feedback equivalent system to our goal system, which can be any sufficiently smooth arbitrary nonlinear function. The former is useful in the current research, as we know that the spider uses the web vibration, i.e. introduces feedback to the system, for structural monitoring and communication. Besides, studying the web deformation modes and web building strategies can give us a framework for designing morphological computational setups.

The theoretical framework and results, discussed in this research, help us with identifying the signal processing properties of spider webs and their possible roles as elements of a morphological computational setup. The identified properties can be used to design new vibration sensors with application in structural health or fluid flow monitoring. The possible morphological computational setup inspires a structural design to outsource the computational burden of signal processing and conditioning, needed to analyze the sensor readings, on the sensor embodiment and morphology. Finally, the relative importance and trade-off between signal processing and pray capturing capabilities of the web structure remain to be investigated further in a future research.

4 Conclusion

This paper describes our approach and presents preliminary results for investigating computational properties of the spider web. A naturally spun spider orb web is experimentally and analytically investigated as the real part of a morphological computation setup, based on the definition of a physical computational system, in response to transverse step inputs. A lumped system model is derived based on the parameters of an earlier FEM model as theoretical part of the morphological computation setup. The web transverse and longitudinal signal filtering, attenuation, delay, memory effect, and deformation modes are briefly discussed. Furthermore, the importance of considering the web frequency filtering and the web hub dynamics are elaborated. Our modeling effort aims to identify and theoretically realize possible computational properties of the web for formulating a dynamic system and an interpretation for this interesting structure as a morphological computation setup. Two potential candidates for such interpretation and dynamic system are identified for (i) a nonlinear time-invariant filter with fading memory, and (ii) autonomous generation of adaptive periodic patterns. However, further investigation in these directions will be carried in the future. The goal is to infer design guidelines for novel types of vibration and flow sensors capable of using their morphological features to carry out relevant computations. To this effect, we plan to build prototypes of such sensors and, inspired by spiders, also physical robots that are capable of deploying such sensors on demand.

5 Acknowledgment

This work is supported by the Leverhulme Trust Research Project, "Computing with spiders' web", number RPG-2016-345, granted to H.H. and F.V.; and the Royal Academy of Engineering (research fellowship RF1516/15/11), granted to L.R. With special thanks to Dr. Helmut Hauser, Dr. Ludovic Renson, Dr. Beth Mortimer, Prof. Fritz Vollrth, Dr. S. Elnaz Naghibi and Alan Quille who contribute to this research by helpful discussions, exchanging ideas, proofreading the draft and providing helpful comments.

References

1. F. Vollrath and P. Selden, "The Role of Behavior in the Evolution of Spiders, Silks, and Webs," *Annual Review of Ecology, Evolution, and Systematics*, vol. 38, no. 1, pp. 819–846, 2007.
2. F. Vollrath, "Coevolution of behaviour and material in the spiders web," *Biomechanics in Animal Behaviour*, pp. 315–29, 2000.
3. U. Slotta, S. Hess, K. Spie, T. Stromer, L. Serpell, and T. Scheibel, "Spider Silk and Amyloid Fibrils: A Structural Comparison," *Macromolecular Bioscience*, vol. 7, no. 2, pp. 183–188, 2007.
4. J. Guan, F. Vollrath, and D. Porter, "Two Mechanisms for Supercontraction in Nephila Spider Dragline Silk," *Biomacromolecules*, vol. 12, pp. 4030–4035, Nov. 2011.
5. W. M. Masters and H. Markl, "Vibration Signal Transmission in Spider Orb Webs," *Science*, vol. 213, pp. 363–365, July 1981.
6. F. G. Barth and Geethabali, "Spider vibration receptors: Threshold curves of individual slits in the metatarsal lyriform organ," *J. Comp. Physiol.*, vol. 148, pp. 175–185, June 1982.
7. B. Mortimer, A. Soler, C. R. Siviour, R. Zaera, and F. Vollrath, "Tuning the instrument: sonic properties in the spider's web," *J R Soc Interface*, vol. 13, Sept. 2016.
8. B. Mortimer, A. Soler, C. R. Siviour, and F. Vollrath, "Remote monitoring of vibrational information in spider webs," *The Science of Nature*, vol. 105, 2018.
9. Y. Aoyanagi and K. Okumura, "Simple Model for the Mechanics of Spider Webs," *Physical Review Letters*, vol. 104, Jan. 2010.
10. A. Soler and R. Zaera, "The secondary frame in spider orb webs: the detail that makes the difference," *Scientific Reports*, vol. 6, p. 31265, Aug. 2016.
11. W. M. Masters, "Vibrations in the Orbwebs of Nuctenea sclopetaria (Araneidae): I. Transmission through the Web," *Behavioral Ecology and Sociobiology*, vol. 15, no. 3, pp. 207–215, 1984.
12. W. M. Masters, "Vibrations in the Orbwebs of Nuctenea sclopetaria (Araneidae): II. Prey and Wind Signals and the Spider's Response Threshold," *Behavioral Ecology and Sociobiology*, vol. 15, no. 3, pp. 217–223, 1984.
13. A. O. Krushynska, F. Bosia, M. Miniaci, and N. M. Pugno, "Tunable spider-web inspired hybrid labyrinthine acoustic metamaterials for low-frequency sound control," *New Journal of Physics*, vol. 19, p. 105001, Oct. 2017. arXiv: 1701.07622.
14. H. Hauser, R. M. Füchslin, and R. Pfeifer, *Opinions and Outlooks on Morphological Computation.* E-Book, 2014.

15. K. Nakajima, T. Li, H. Hauser, and R. Pfeifer, "Exploiting short-term memory in soft body dynamics as a computational resource," *Journal of The Royal Society Interface*, vol. 11, p. 20140437, Nov. 2014.
16. K. Nakajima, H. Hauser, T. Li, and R. Pfeifer, "Information processing via physical soft body," *Scientific Reports*, vol. 5, p. 10487, May 2015.
17. H. Hauser, A. J. Ijspeert, R. M. Füchslin, R. Pfeifer, and W. Maass, "The role of feedback in morphological computation with compliant bodies," *Biol Cybern*, vol. 106, pp. 595–613, Nov. 2012.
18. H. Hauser, A. J. Ijspeert, R. M. Füchslin, R. Pfeifer, and W. Maass, "Towards a theoretical foundation for morphological computation with compliant bodies," *Biol Cybern*, vol. 105, pp. 355–370, Dec. 2011.
19. R. Pfeifer and J. Bongard, *How the Body Shapes the Way We Think: A New View of Intelligence*. MIT Press, Oct. 2006. Google-Books-ID: EHPMv9MfgWwC.
20. N. Sornkarn, M. Howard, and T. Nanayakkara, "Internal impedance control helps information gain in embodied perception," *Proceedings - IEEE International Conference on Robotics and Automation*, pp. 6685–6690, 2014. 00000.
21. S. Sadati, L. Sullivan, I. Walker, K. Althoefer, and T. Nanayakkara, "Three-Dimensional-Printable Thermoactive Helical Interface With Decentralized Morphological Stiffness Control for Continuum Manipulators," *IEEE Robotics and Automation Letters*, vol. 3, pp. 2283–2290, July 2018.
22. Q. Zhao, K. Nakajima, H. Sumioka, H. Hauser, and R. Pfeifer, "Spine dynamics as a computational resource in spine-driven quadruped locomotion," in *2013 IEEE/RSJ International Conference on Intelligent Robots and Systems*, pp. 1445–1451, Nov. 2013.
23. K. Ghazi-Zahedi, D. F. B. Haeufle, G. Montfar, S. Schmitt, and N. Ay, "Evaluating Morphological Computation in Muscle and DC-Motor Driven Models of Hopping Movements," *Front. Robot. AI*, vol. 3, 2016.
24. K. Ghazi-Zahedi, C. Langer, and N. Ay, "Morphological Computation: Synergy of Body and Brain," *Entropy*, vol. 19, p. 456, Aug. 2017.
25. R. M. Füchslin, A. Dzyakanchuk, D. Flumini, H. Hauser, K. J. Hunt, R. H. Luchsinger, B. Reller, S. Scheidegger, and R. Walker, "Morphological Computation and Morphological Control: Steps Toward a Formal Theory and Applications," *Artificial Life*, vol. 19, pp. 9–34, Nov. 2012.
26. M. Giunti, *Computation, Dynamics, and Cognition*. Oxford University Press, June 1997.
27. M. Giunti, "What is a physical realization of a computational system?," *ISONOMIA*, vol. 9, no. Epistemologica Series, Special Issue: Reasoning, Metaphor and Science, pp. 177–192, 2017.
28. S. Sadati, S. Naghibi, and M. Naraghi, "An Automatic Algorithm to Derive Linear Vector Form of Lagrangian Equation of Motion with Collision and Constraint," *Procedia Computer Science*, vol. 76, pp. 217–222, 2015.
29. S. Sadati, "AutoTMTDyn Software Package," May 2017. https://github.com/hadisdt/AutoTMTDyn.